Journal of Applied Physics

Temperature dependence of broadband near-infrared luminescence from Ni^{2+}-doped $Ba_{0.5}Sr_{0.5}TiO_3$

Cite as: J. Appl. Phys. **118**, 183110 (2015); https://doi.org/10.1063/1.4935637
Submitted: 10 September 2015 . Accepted: 02 November 2015 . Published Online: 12 November 2015

Gongxun Bai, Wenjing Jie, Zhibin Yang, and Jianhua Hao

Temperature dependence of broadband near-infrared luminescence from Ni^{2+}-doped $Ba_{0.5}Sr_{0.5}TiO_3$

Gongxun Bai,[1,2] Wenjing Jie,[1,2] Zhibin Yang,[1,2] and Jianhua Hao[1,2,a)]
[1]*Department of Applied Physics, The Hong Kong Polytechnic University, Hong Kong, People's Republic of China*
[2]*Shenzhen Research Institute, The Hong Kong Polytechnic University, Shenzhen 518057, People's Republic of China*

(Received 10 September 2015; accepted 2 November 2015; published online 12 November 2015)

The dielectric and photoluminescence properties of Ni^{2+}-doped $Ba_{0.5}Sr_{0.5}TiO_3$ (BST) were studied at different temperatures. Under 350 nm excitation, the NIR luminescence band from 1200 nm to >1600 nm covers the optical communication window (O-L bands), with a typical bandwidth exceeding 200 nm. The crystal structure of Ni^{2+}-doped BST evolves from rhombohedral to cubic when the temperature increases from 100 to 300 K. The luminescence properties are tightly correlated with the crystal structure of the host BST. The luminescence variations are mainly affected by phase transition induced crystal field change and nonradiative relaxation. © *2015 AIP Publishing LLC*. [http://dx.doi.org/10.1063/1.4935637]

INTRODUCTION

The ever-increasing demand in medical, energy, optical communication, and many other applications has raised an expanding requirement for near-infrared (NIR) luminescence materials.[1–4] Recently, 3*d* transition metal ions Ni^{2+} doped NIR luminescence materials have attracted considerable attention due to their broadband emission covering the whole optical fiber communication window.[5] Up to now, various types of Ni^{2+} doped NIR luminescence materials, such as glass ceramics and crystals, have been developed due to their potential applications in tunable lasers and broadband optical amplifiers.[6,7] It is known that tailoring the host chemical composition of Ni^{2+} can effectively modulate the NIR luminescence, due to the variation in local ligand field around active ions. Therefore, it is very interesting to investigate whether the tuning of luminescence can be achieved in one fixed host.

On the other hand, perovskite oxides are an important class of dielectric materials, which have widely been used in microwave devices, smart sensors, and piezoelectric transducers.[8–10] Particularly, active ions doped barium strontium titanate has drawn great attention for its simultaneous ferroelectric and optical properties,[11,12] suggesting attractive applications in multifunctional optoelectronic devices.[3,13] Recently, our research group reported tunable and ultrabroadband NIR luminescence from Ni^{2+}-doped ferroelectric perovskites.[14] In particular, the full width at half maximum (FWHM) of Ni^{2+}-doped $Ba_{0.5}Sr_{0.5}TO_3$ (BST) reached as large as 295 nm at room temperature. It is known that dielectric properties of BST depend on the temperature, ascribed to the evolution of crystal structure. Although the temperature dependent structural and electrical properties of these BST have been extensively explored for applications in tunable devices.[15] Studies about temperature dependent photoluminescence (PL) from luminescent BST have been seldom reported until now. Since the electron transitions among *d* orbits of Ni^{2+} ion are very sensitive to the matrixes,[14,16] the luminescence could be strongly affected by the phase transition. Hence, it is interesting to investigate the relationship between the luminescence of Ni^{2+}-doped BST and temperature. In this letter, temperature dependent PL from Ni^{2+}-doped BST will be presented.

EXPERIMENTAL

The Ni^{2+}-doped BST powder was prepared by solid state chemical reaction method. Analytical grade NiO, $BaCO_3$, $SrCO_3$, and TiO_2 powders were used as raw materials. These powders were weighted according to the molecular formula $Ba_{0.5}Sr_{0.5}Ti_{0.995}Ni_{0.005}O_3$. Here, the Ti^{4+} site was substituted by Ni^{2+}, and the charge neutrality could be maintained by the formation of oxygen vacancies. The starting powders with designed stoichiometric amounts were ball milled for 24 h, then dried and calcined at 1100 °C for 8 h in air. The resulting powders were pressed into disc samples with 10 mm diameter × 0.5 mm thick, and sintered at 1350 °C for 4 h in air. Using the prepared disc as target, Ni^{2+}-doped BST thin films were grown on (100) $LaAlO_3$ (LAO) single crystal substrates by pulsed laser deposition method. The BST film was deposited with the growth temperature of 700 °C and oxygen pressure of 20 Pa.

The X-ray diffraction (XRD) patterns of the BST powder and thin film were recorded by an X-ray diffractometer (Rigaku, SmartLab). The dielectric properties of BST disc were measured by using an HP 4294A impedance analyzer connected to an Oxford temperature controlled chamber (80 K–300 K). Temperature-dependent PL analyses (100–300 K) were performed in a closed-cycle liquid helium cryostat. The PL and photoluminescence excitation (PLE) spectra were measured using an Edinburgh FLSP920 spectrophotometer equipped with a nitrogen-cooled NIR photomultiplier tube (Hamamatsu C9940–02) and a 450 W steady-state

a)Author to whom correspondence should be addressed. Electronic mail: jh.hao@polyu.edu.hk.

xenon lamp. Meanwhile, the decay curves were recorded with a pulsed 60 W Xe flashlamp.

RESULTS AND DISCUSSION

Figure 1(a) presents the XRD pattern of Ni^{2+}-doped BST powder at room temperature. A standard BST ceramic pattern was observed without any secondary impurity phases, indicating that Ni^{2+} ions were efficiently doped into the BST host lattice. The temperature dependent dielectric constant of Ni^{2+}-doped BST disc at the frequency of 1 kHz is shown in Figure 1(b). One can observe three local maximum dielectric constants corresponding to three phase transitions: a weak peak locates at about 144 K which corresponds to the phase transition from rhombohedral (3m) to orthorhombic (mm2). The weak peak locates around 178 K indicating the phase transition from orthorhombic (mm2) to tetragonal (4 mm). A remarkable peak around 216 K is corresponding to the phase transition from tetragonal (4 mm) to cubic (m3m). Thus the Curie temperature (T_c) of Ni^{2+}-doped BST is 216 K. The behaviours are similar to the previous reports of undoped BST bulk sample,[17] indicating that activator Ni^{2+} seems to have little effect on the dielectric property of BST disc.

NIR PLE spectra of Ni^{2+}-doped BST sample are presented in Figure 2(a) as a function of temperature. The PLE spectra were recorded by monitoring PL at 1350 nm. The most intense excitation band of BST sample is located at

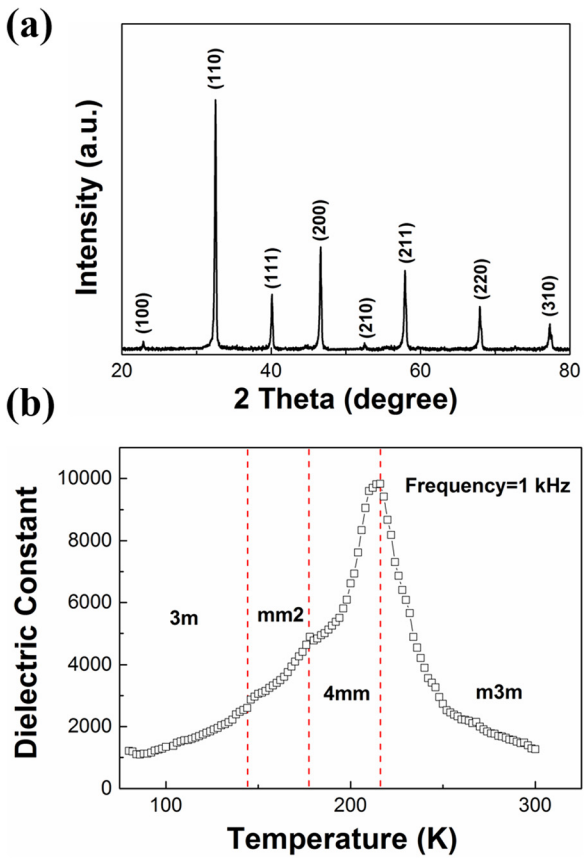

FIG. 1. (a) XRD pattern of Ni^{2+}-doped BST powder in the 2θ scan range of 20°–80°. (b) Temperature dependent dielectric constant of Ni^{2+}-doped BST disc.

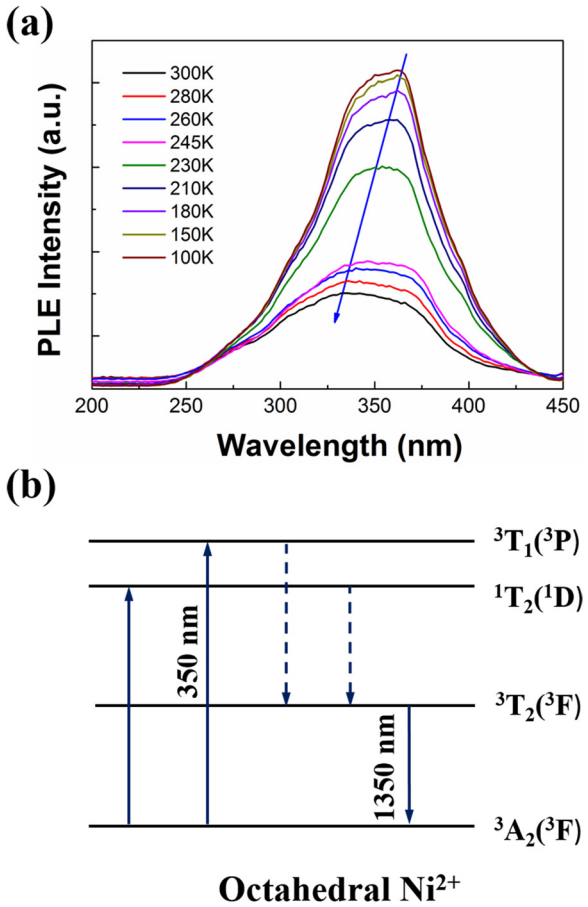

FIG. 2. (a) Temperature dependent PLE spectra of Ni^{2+}-doped BST disc, $\lambda_{em} = 1350$ nm. (b) Energy levels and transitions of Ni^{2+} in octahedral sites.

about 350 nm, which can be assigned to spin-allowed $^{VI}Ni^{2+}$: $^3T_1(^3P) \rightarrow {}^3A_2(^3F)$ [Figure 2(b)]. With increasing temperature, the excitation peak shows a slight blue shift, covering the spectral range of 250–450 nm. It matches well emitting band of UV LED (250–400 nm). Therefore, commercial UV LED can be used as potential pumping sources. Temperature dependent NIR PL spectra were recorded under excitation at 350 nm [Figure 3(a)]. The resulting emission spectra are dominated by broad bands (from 1200 to >1600 nm) which peak at about 1350 nm. In particular, FWHM of these bands exceeds 200 nm. The PL results do not beyond 1600 nm are due to the low spectral response of the InGaAs detector at around 1600 nm. NIR PL originates from the spin-allowed relaxation of $^{VI}Ni^{2+}$:$^3A_{2g}(^3F) \rightarrow {}^3T_{1g}(^3P)$ [Figure 2(b)] and covers the whole optical communication window (O-L bands). As shown in Figure 3(b), integrated intensity and position of PL bands remain unchanged when temperature is below 150 K. The changes of PL intensity and peak position are very small when temperature is below 180 K. As increasing temperature from 180 K to 210 K, the PL intensity gradually decreases and the emission peak shows a visible redshift. Around 230 K, both PL intensity and position present a remarkable change. And then the emission intensity decreases continually and the PL peak red shifts steadily by raising temperature gradually. Meanwhile, FWHM obviously becomes broaden when temperature arises above 230 K [Figure 3(a)]. Notably, unlike the significant decrease in the emission

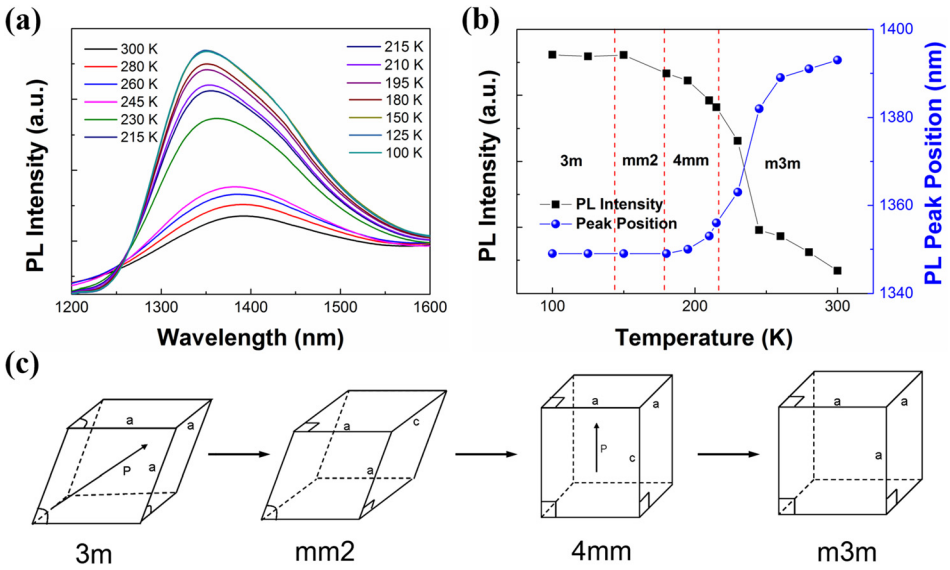

FIG. 3. (a) Temperature dependent PL spectra of Ni^{2+}-doped BST disc, $\lambda_{ex} = 350$ nm. (b) PL intensity and peak position of Ni^{2+}-doped BST disc as a function of temperature changed from 100 K to 300 K. (c) Phase transition of Ni^{2+}-doped BST.

intensity previously recorded in Ni^{2+}-doped glass,[18] the PL intensity of our samples at 300 K is still about 50% as strong as that at 100 K, suggesting less thermal quenching in BST ceramics at room temperature. Differing from Ni^{2+}-doped glass ceramics,[19] a redshift occurs as increasing temperature, namely, from 1350 nm at 100 K to 1393 nm at 300 K. According to the above discussion in Figure 1(b), the NIR PL change could be finely explained by the phase transitions of Ni^{2+}-doped BST under different temperatures. As shown in Figure 3(c), below 144 K, the phase of Ni^{2+}-doped BST sample keeps rhombohedral (3m), without PL change. As raising temperature from 144 K to 178 K, the phase maintaining orthorhombic (mm2), the PL intensity slightly decreases and peak position almost unchanges. The slight PL change below 178 K can be attributed to little crystal field change when phase transition from rhombohedral (3m) to orthorhombic (mm2). When increasing temperature from 178 K to 300 K, the PL peak position presents a red shift, due to the weaken crystal field around Ni^{2+} ions.[16] The decreasing PL intensity could be ascribed to the enhanced temperature dependent nonradiative relaxation.[20] In particular, considerable emission change around T_c is due to the phase transition from tetragonal (4 mm) to cubic (m3m). Therefore, the luminescence behaviours of Ni^{2+} ions could be used to record the phase transition of BST.

The normalized NIR PL decay curves at different temperatures are presented in Figure 4, recording PL intensity at 1350 nm under the excitation at 350 nm. None of the decay curves appears to follow a single exponential equation. Non-exponential characteristic of the decay curve of Ni^{2+}-doped BST might ascribe to the variation of environment surrounding Ni^{2+} ions since the BST micro crystal sizes generally not the same.[21] At the temperature below 230 K, the PL decay slightly varies. It can be deduced to the weak electron-phonon coupling[20] and nonradiative relaxation when temperature is below T_c. The PL decay gradually becomes rapid when temperature is increasing from 230 K to 300 K. This suggests that decay of Ni^{2+}-doped BST is more sensitive to temperature in cubic (m3m) phase. Internal quantum efficiency η of the NIR PL process at temperature $T = x$ can be obtained from $\eta_T = x = (\tau_x/\tau_{5\,K}) \times 100$, where τ_x is the experimental lifetime as obtained at temperature x and $\tau_{5\,K}$ is the extrapolated lifetime at 5 K.[19] For our sample at ambient temperature ($x = 300$ K), a value of $\eta = 49\%$ was obtained. The effective lifetime τ can be obtained from Figure 4 when the emission intensity falls to $1/e$ of its initial value. τ at 100 K was found about 327 μs. Its value decreases to 160 μs at 300 K, due to the temperature dependent nonradiative relaxation in $^{VI}Ni^{2+}$:$^3A_{2g}(^3F) \rightarrow {}^3T_{1g}(^3P)$. The measured lifetime (160 μs) at 300 K is much longer than that of Ni^{2+}-doped Ba-Al titanate glass ceramics (39 μs).[19] The longer lifetime is beneficial for application in mode locked lasers.

In the above experiments, ultrabroadband NIR PL is demonstrated in BST ceramics. Compared with bulk materials, the utilization of a thin film structure facilitates the fabrication and integration of photonic devices.[22] Figure 5(a) shows XRD pattern of as-prepared Ni^{2+}-doped BST thin film (1200 nm) grown on LAO substrate. It is known that LAO can be widely utilized as substrate to fabricate dielectric and ferroelectric thin films.[23] In the θ–2θ scan, only BST (100), (200) and LAO (100), (200) peaks were observed. No other peaks were present. This indicates that the Ni^{2+}-doped

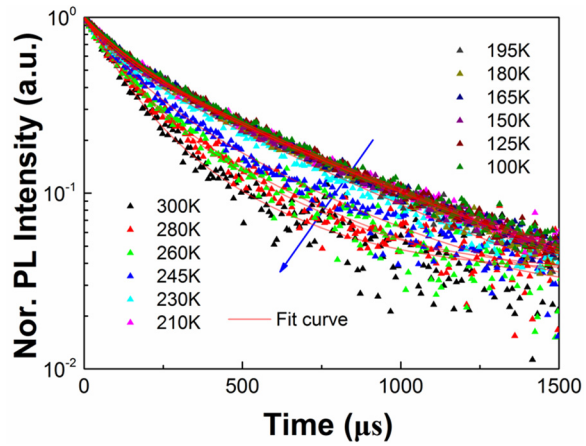

FIG. 4. PL decay curves of Ni^{2+}-doped BST disc at different temperatures, $\lambda_{ex} = 350$ nm and $\lambda_{em} = 1350$ nm.

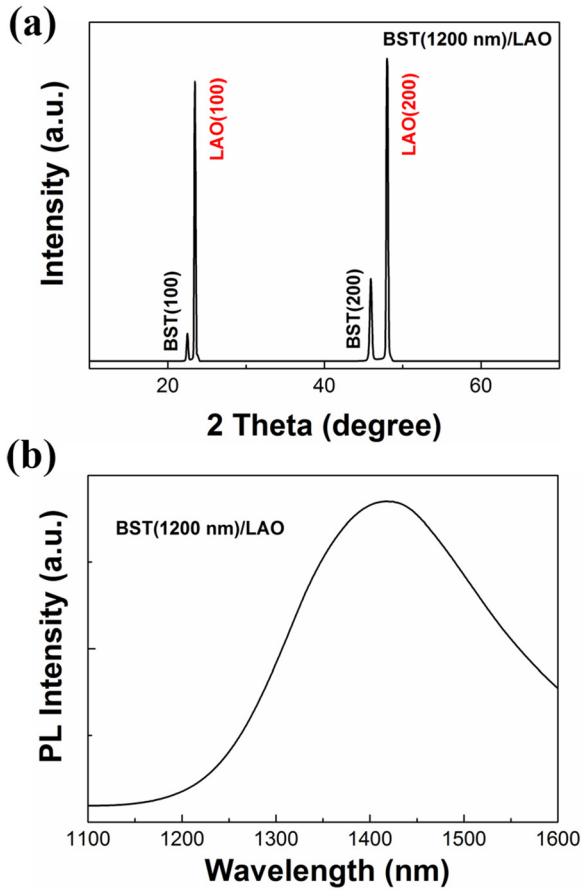

FIG. 5. (a) XRD pattern of Ni^{2+}-doped BST(1200 nm)/LAO sample. (b) PL spectrum of Ni^{2+}-doped BST(1200 nm)/LAO sample.

BST thin film is highly oriented grown on (100) LAO substrate. Figure 5(b) presents the NIR PL spectrum of Ni^{2+}-doped BST(1200 nm)/LAO sample at room temperature, under 350 nm excitation. The NIR emission band peaks locate at about 1418 nm, with a broad width (FWHM) exceeding 260 nm. The ultrabroadband NIR emission covers the whole telecommunication window. The result suggests that the developed Ni^{2+}-doped BST/LAO is potentially promising for various applications as a broadband gain medium for optical amplifier and optoelectronic integrated devices.

CONCLUSION

In conclusion, ultrabroadband NIR luminescence from Ni^{2+}-doped BST is demonstrated. With the increase of temperature, the luminescence properties are affected by phase transition induced crystal field change and temperature dependent nonradiative relaxation. Ni^{2+} ions can be a promising probe for the crystal structure at low temperature (below 230 K). The broadband NIR PL covers optical communication band from 1200 nm to >1600 nm, with a bandwidth greater than 200 nm. The excited state lifetime of $^{VI}Ni^{2+}$:$^3T_2(^3F)$ was found to be 327 μs at 100 K and 160 μs at 300 K. In addition, ultrabroadband NIR luminescence was also observed in Ni^{2+}-doped BST thin film at ambient temperature. The presented results make Ni^{2+}-doped BST promising for widespread applications in broadband optical amplifier and optoelectronic integrated devices.

ACKNOWLEDGMENTS

The research was financially supported by the grants from Research Grants Council of Hong Kong (GRF No. PolyU 5002/12P), National Natural Science Foundation of China (No. 51272218), Shenzhen Matching Grant (No. R2013A062), and PolyU Matching Grant for China Projects (No. 4-BCAG).

[1]M. Smith, M. C. Mancini, and S. Nie, Nat. Nanotechnol. **4**, 710 (2009).
[2]G. X. Bai, M.-K. Tsang, and J. H. Hao, Adv. Opt. Mater. **3**, 431 (2015).
[3]M.-K. Tsang, G. X. Bai, and J. H. Hao, Chem. Soc. Rev. **44**, 1585 (2015).
[4]B. Xu, J. H. Hao, Q. B. Guo, J. C. Wang, G. X. Bai, B. Fei, S. F. Zhou, and J. R. Qiu, J. Mater. Chem. C **2**, 2482 (2014).
[5]S. F. Zhou, N. Jiang, B. T. Wu, J. H. Hao, and J. R. Qiu, Adv. Funct. Mater. **19**, 2081 (2009).
[6]S. F. Zhou, J. H. Hao, and J. R. Qiu, J. Am. Ceram. Soc. **94**, 2902 (2011).
[7]S. F. Zhou, N. Jiang, H. F. Dong, H. P. Zeng, J. H. Hao, and J. R. Qiu, Nanotechnology **19**, 015702 (2008).
[8]Z. P. Wu, W. Huang, K. H. Wong, and J. H. Hao, J. Appl. Phys. **104**, 054103 (2008).
[9]Z. B. Yang and J. H. Hao, J. Appl. Phys. **112**, 054110 (2012).
[10]J. H. Hao, W. Si, X. X. Xi, R. Guo, A. Bhalla, and L. Cross, Appl. Phys. Lett. **76**, 3100 (2000).
[11]Y. Zhang, J. H. Hao, C. L. Mak, and X. H. Wei, Opt. Express **19**, 1824 (2011).
[12]K. B. Ruan, G. H. Wu, H. Zhou, and D. H. Bao, J. Electroceram. **29**, 37 (2012).
[13]J. H. Hao, Y. Zhang, and X. H. Wei, Angew. Chem., Int. Ed. **123**, 7008 (2011).
[14]G. X. Bai, Y. Zhang, and J. H. Hao, J. Mater. Chem. C **2**, 4631 (2014).
[15]V. Lemanov, E. Smirnova, P. Syrnikov, and E. Tarakanov, Phys. Rev. B **54**, 3151 (1996).
[16]G. Bai, Y. Zhang, and J. Hao, Sci. Rep. **4**, 5724 (2014).
[17]L. Z. Cao, B. L. Cheng, S. Y. Wang, W. Y. Fu, S. Ding, Z. H. Sun, H. T. Yuan, Y. L. Zhou, Z. H. Chen, and G. Z. Yang, J. Phys. D: Appl. Phys. **39**, 2819 (2006).
[18]T. Suzuki and Y. Ohishi, Appl. Phys. Lett. **84**, 3804 (2004).
[19]G. J. Gao, M. Y. Peng, and L. Wondraczek, Opt. Lett. **37**, 1166 (2012).
[20]M. G. Brik, J. Phys. Chem. Solids **67**, 738 (2006).
[21]B. T. Wu, N. Jiang, S. F. Zhou, D. P. Chen, C. S. Zhu, and J. R. Qiu, Opt. Mater. **30**, 1900 (2008).
[22]Y. Zhang and J. H. Hao, J. Mater. Chem. C **1**, 5607 (2013).
[23]Y. B. Zheng, S. J. Wang, L. B. Kong, S. Tripathy, A. C. H. Huan, and C. K. Ong, J. Electroceram. **16**, 571 (2006).